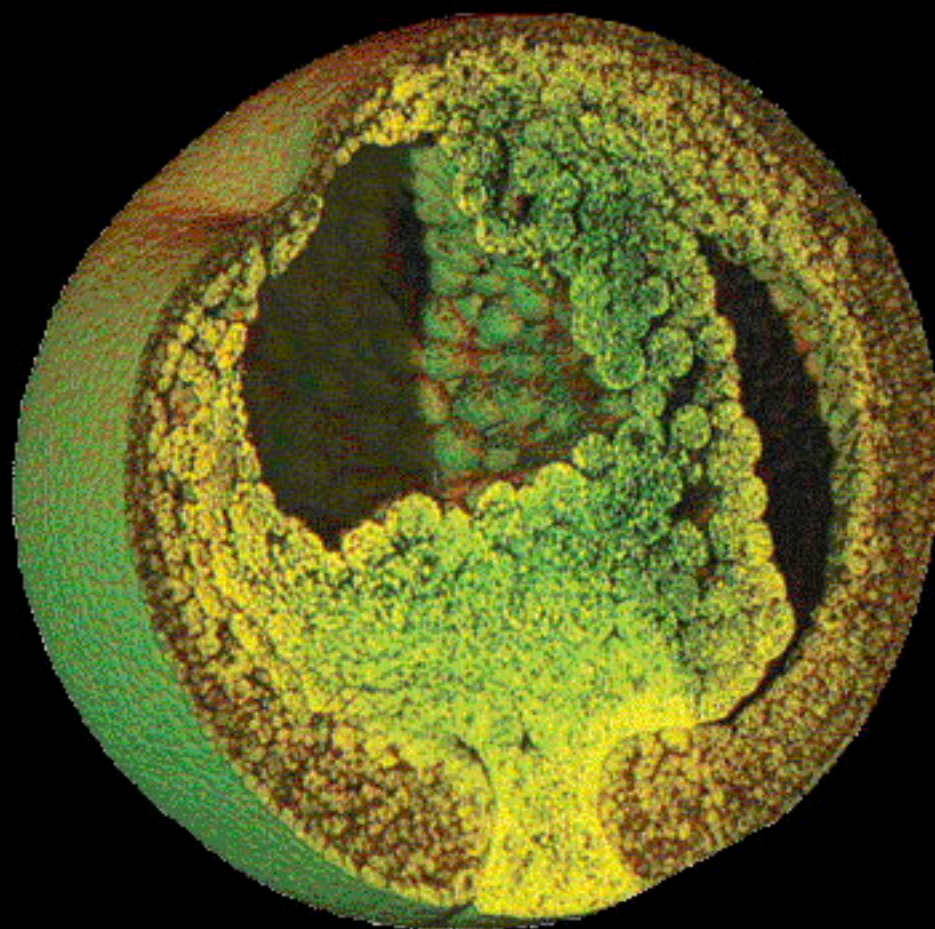


DEVELOPMENTAL DYNAMICS

*An Official Publication of the
American Association of Anatomists*

Volume 225, Number 3, November 2002

Articles published online in Wiley InterScience, 24 September 2002–xx October 2002



WILEY-LISS
ISSN 1058-8388

Wiley InterScience
Early View
WILEY-LISS

BRIEF COMMUNICATIONS

Surface Imaging Microscopy, An Automated Method for Visualizing Whole Embryo Samples in Three Dimensions at High Resolution

ANDREW J. EWALD,¹ HELEN MCBRIDE,¹ MARK REDDINGTON,² SCOTT E. FRASER,^{1*}
AND RUSSELL KERSCHMANN²

¹Biological Imaging Center and Division of Biology, Caltech, Pasadena, California

²Resolution Sciences Corporation, Corte Madera, California

ABSTRACT Modern biology is faced with the challenge of understanding the specification, generation, and maintenance of structures ranging from cells and tissues to organs and organisms. By acquiring images directly from the block face of an embedded sample, surface imaging microscopy (SIM) generates high-resolution volumetric images of biological specimens across all of these scales. Surface imaging microscopy expands our range of imaging tools by generating three-dimensional reconstructions of embryo samples at high resolution and high contrast. SIM image quality is not limited by depth or the optical properties of overlying tissue, and intrinsic or extrinsic alignment markers are not required for volume reconstruction. These volumes are highly isotropic, enabling them to be virtually sectioned in any direction without loss of image quality. Surface imaging microscopy provided a more accurate three-dimensional representation of a chick embryo than confocal microscopy of the same sample. SIM offers excellent imaging of embryos from three major vertebrate systems in developmental biology: mouse, chicken, and frog. Immediate applications of this technology are in visualizing and understanding complex morphogenetic events and in making detailed comparisons between normal and genetically modified embryos. © 2002 Wiley-Liss, Inc.

Key words: three-dimensional reconstruction; morphogenesis; anatomy; visualization; imaging; frog; mouse; chicken

INTRODUCTION

Motivation

We are interested in understanding the way in which cellular function and behavior generate structures of high complexity, such as tissues and organs. The most logical structure around which to organize and synthesize these different categories of information is the three-dimensional (3D) anatomy of the specimen. In

short, we must know both where and when an event occurs before we can understand how it occurs. Such an effort will require imaging techniques spanning several orders of magnitude in spatial and temporal resolution. Current imaging techniques provide tools for high-resolution imaging of small volumes or low-resolution imaging of large volumes. A technique is needed to bridge this gap. Surface imaging microscopy meets this need.

Properties of the Basic Technique

Surface imaging microscopy (SIM) is an automated imaging technique that captures fluorescence images from the freshly cut surface of an opaque polymer block. The microscope is composed of an integrated microtome and widefield fluorescence microscope, with a computer controlled translation stage that holds the embedded sample, draws it over a diamond knife, and returns the sample to the field of view of the objective lens. Images can be collected into one, two, or three independent fluorescent channels, and the signal can be either the inherent autofluorescence of the tissue or the extrinsic contrast supplied by a fluorescent dye.

The depth of field in a SIM image is set by the amount of opacifier added to the embedding polymer. This amount can be empirically tuned to closely match the in-plane resolution of the image through the range of magnification of 2–40× microscope objectives, corresponding to 8.8–0.4 micron resolution and sample sizes from 8–0.5 mm. The resulting SIM data set is nearly isotropic, as the in-plane resolution of the microscope objective lens is matched to the thickness of the sections removed and to the depth of field of the

Grant sponsor: NIH NRSA; Grant number: 5 F32 NS10941.
Dr. Reddington's present address is Biosearch Technologies, Inc., 81 Digital Drive, Novato, CA 94949.

*Correspondence to: Scott E. Fraser, Biological Imaging Center and Division of Biology, Caltech, Mail Code 139-74, Pasadena, CA 91125.
E-mail: sefraser@caltech.edu

Received 2 July 2001; Accepted 28 August 2002

DOI 10.1002/dvdy.10169

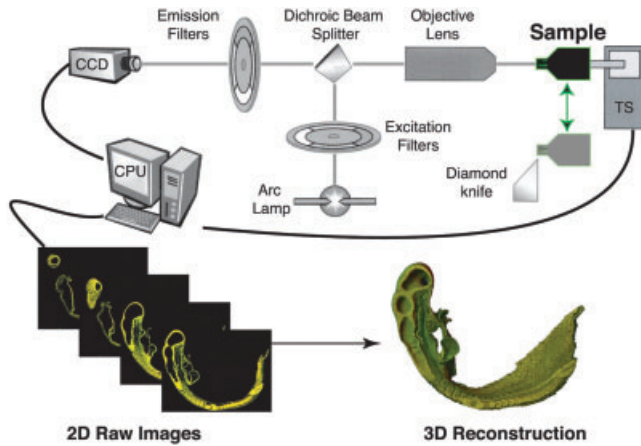


Fig. 1. Description of the basic technique. Schematic depiction of surface imaging microscopy (SIM). A fluorescently labeled specimen is fixed, labeled, dehydrated, infiltrated, and embedded in a black polymer, then loaded onto a motorized translation stage (TS). A computer (CPU) controls and synchronizes the movement of the sample over a diamond knife, removing a thin section of material and returning the sample to the field of view of an objective lens. An image of the surface of the block is collected by a charge-coupled device (CCD) camera, and the process repeats. This aligned series of two-dimensional images can then be reassembled computationally into a three-dimensional volume in standard image processing applications.

image as determined by the penetration depth of light into the sample. The field of view of the microscope objective determines the in-plane sample size, but there is no inherent limit to the total depth of the specimen that can be sampled. The immediate output of SIM is a registered series of two-dimensional (2D) images, which are then computationally reconstructed into a 3D volume. The realignment accuracy of the stage is sufficient that the misregistration between subsequent images is subresolution and no post hoc realignment is necessary. Figure 1 schematically depicts a surface imaging microscope.

RESULTS AND DISCUSSION

Quality of 2D Images

Figure 2 depicts three orthogonal views through a typical SIM data set of a chick embryo (stained with Resolution Standard stain). The main panel is the raw x - y image collected from the block surface. The x - y view demonstrates that the raw images of a SIM data set have high contrast, high resolution, and excellent tissue preservation. Additionally, the embryo is clearly distinct from the surrounding block, greatly facilitating

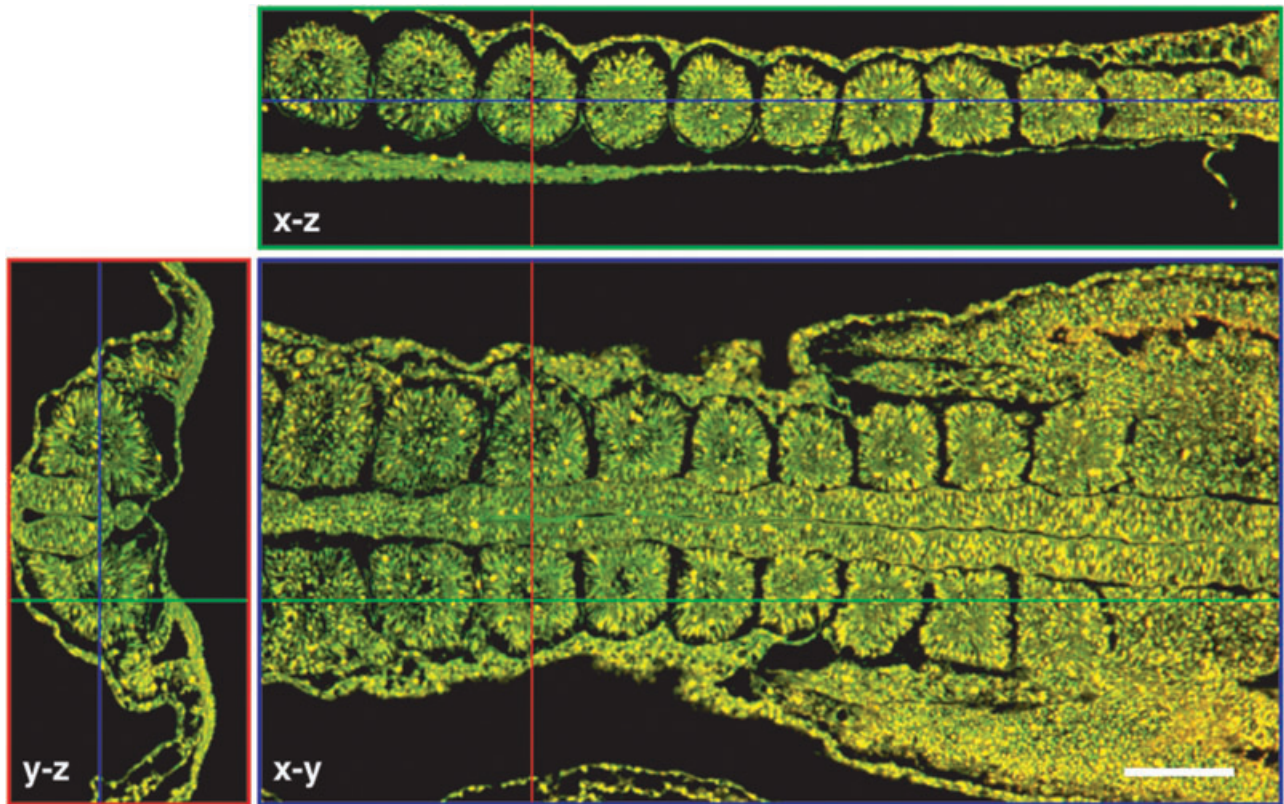


Fig. 2. Evaluation of image and data set quality. Two-dimensional data resulting from a surface imaging microscopy (SIM) data set of a fluorescently labeled chick trunk, stained with Resolution Standard stain (Resolution Sciences Corporation). Anterior is to the left. Note in particular the similarity in contrast, resolution, and level of detail in the three views. The raw x - y image collected by the charge-coupled device camera corresponds closely to a frontal section through the embryo. This image is a

representative single section from the data set. The red and green lines mark the axial levels at which the orthogonal views were extracted. The x - z view is a computationally reconstructed sagittal view of the data set, highlighting the developmental progression of somites as a function of distance along the anterior-posterior axis. The y - z view is a computationally reconstructed transverse view through the data set, highlighting the neural tube, notochord, and paired somites. Scale bar = 100 microns.

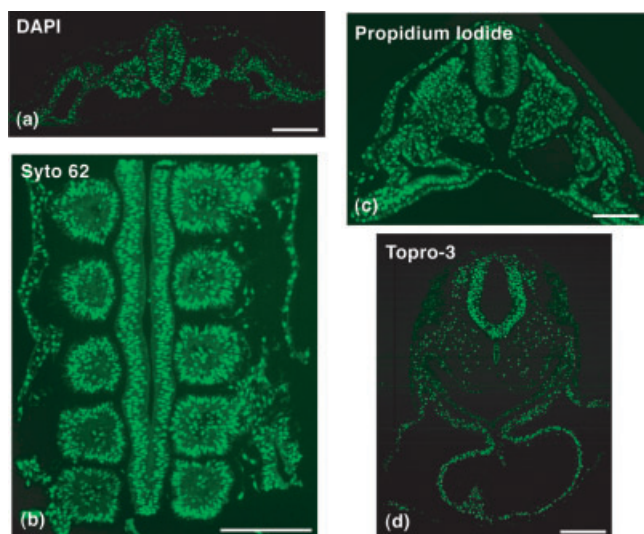


Fig. 3. Surface imaging microscopy (SIM) images of various nuclear dyes. **a:** Transverse section through the trunk of a chick embryo labeled with diamidino-phenyl-indole (DAPI) and imaged using SIM. **b:** Frontal section through the trunk of a chick embryo labeled with Syto 62 and imaged using SIM. **c:** Transverse section through a chick trunk labeled with propidium iodide and imaged using SIM. **d:** Transverse section through rhombomere 4 of a chick hindbrain labeled with Topro-3 and imaged using SIM.

3D reconstructions. It is also evident from the x - y view that there is minimal knife chatter in the image and that SIM captures a wide field of view at cellular resolution. We have collected images of similar quality by using tissue autofluorescence, diamidino-phenyl-indole (DAPI), propidium iodide, Syto 62, and Topro-3 (Molecular Probes, Eugene, OR); Figure 3 shows 2D images acquired with each of these dyes. These dyes range in emission wavelength from the near-ultraviolet through the near-infrared and demonstrate that the embedding polymer and the imaging system are sensitive to the entire visible spectrum.

Quality of Data Sets

Orthogonal sections through the data set are necessary to critically assess many aspects of the quality of SIM data sets; these sections reveal time- and depth-dependent variations in image quality. Figure 2 presents x - z and y - z sections through the same data set, at the levels indicated by the colored lines. Changes in fluorescence excitation intensity or camera efficiency over the course of the imaging would show up in the x - z or y - z sections as lines that were aberrantly brighter or darker than adjacent sections. This artifact is not typically present in SIM data sets. Misregistration of the blockface during imaging would cause smooth curves within features of the data set to appear jagged, as structures that were adjacent in the sample are mistakenly separated in the resulting data set. The contiguous outlines of individual cells and the smooth outlines defining tissue blocks and cavities argues that any registration errors are subresolution. No align-

ment algorithms have been used to process this data set; the registration evident in Figure 2 is indicative of the alignment of the raw data.

SIM relies on staining samples in whole-mount, then imaging thin optical sections of the surface of the sample. As a result the dye needs to penetrate adequately in the whole sample and then be sufficiently bright in the thin optical section. Inconsistencies in dye penetration would show in the x - z and y - z images as changes in color or intensity through structures of similar cellular composition, such as epithelial somites. Figure 2 is clear evidence that our labeling techniques yield uniformly stained samples and that SIM has the sensitivity to detect the fluorescent signal from thin optical sections.

A major technical advantage of SIM over previous blockface imaging efforts (Hegre and Brashear, 1946; Postlethwait, 1962; Odgaard et al., 1990; Weninger and Mohun, 2002) is the isotropicity of the resulting 3D data sets. The axial resolution of any 3D imaging technique is best judged by evaluating x - z and y - z orthogonal sections through the data set. We find the level of resolution, contrast, and detail preserved to be indistinguishable in the three dimensions. Therein lies the major strength of SIM: the in-plane tissue and cavity architecture preservation in SIM is comparable to that achieved in thin paraffin sections or confocal optical sections and its through-plane resolution is currently unrivaled on large, thick samples.

Comparison With Other Imaging Techniques

Current imaging techniques are not well suited to imaging millimeter-scale samples at micron-scale resolutions. Traditional histology has an extensive history of specific stains, both fluorescent and colorimetric, but is quite laborious and requires the viewing and/or photographing of hundreds to thousands of physical sections to gain an appreciation of complex 3D structures. Methods that capture images of these sections and computationally warp them into 3D volumes are of considerable use but have not been reported to have resolution or isotropicity similar to SIM (Streicher et al., 1997; Brune et al., 1999). Previous efforts have also imaged the blockface of samples after physical sectioning, to build 3D reconstructions of samples (Hegre and Brashear, 1946; Postlethwait, 1962; Odgaard et al., 1990; Toga et al., 1996; Weninger and Mohun, 2002). SIM is distinguished from other block face approaches in the resolution, the contrast, and the tissue detail preserved through imaging. SIM resolves cells and subcellular structures and can be used to label specific subpopulations of cells within an embryo, in contrast to lower resolution alternative methods, which rely on the inherent contrast in the tissue (Odgaard et al., 1990; Weninger and Mohun, 2002). Finally, the range of possible sample applications for SIM is broader; we have successfully imaged samples as delicate as early gastrulae chick embryos and samples as rigid as noncalcified trabecular bone.

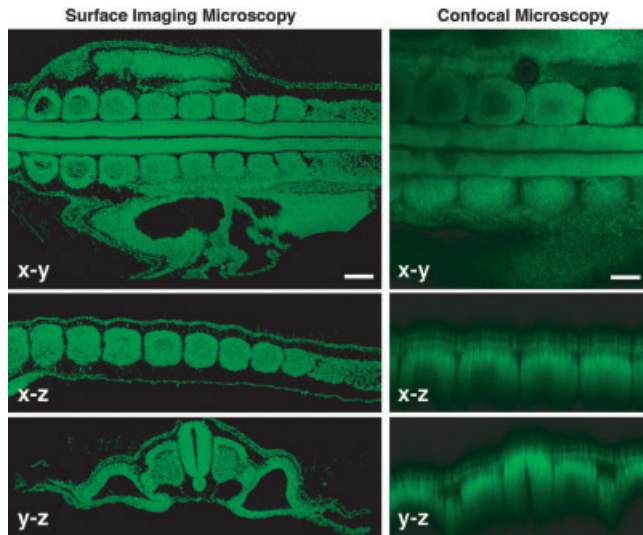


Fig. 4. Comparison of surface imaging microscopy (SIM) with confocal microscopy. Comparative imaging of a chick trunk segment stained with propidium iodide and imaged with both surface imaging microscopy and confocal laser scanning microscopy. Each technique is presented with three orthogonal views, starting with the original (x-y) plane of optical section and following with computationally reconstructed views extracted from the resulting volume. Both data sets were collected with 1.7-micron optical resolution and sections were collected at 1.7-micron intervals. Note in particular the equivalence of the resolution, contrast, and level of detail in the x-y, x-z, and y-z views from the SIM data set and the steep decline in image intensity as a function of depth into the data set in the confocal data set. Scale bar = 100 microns.

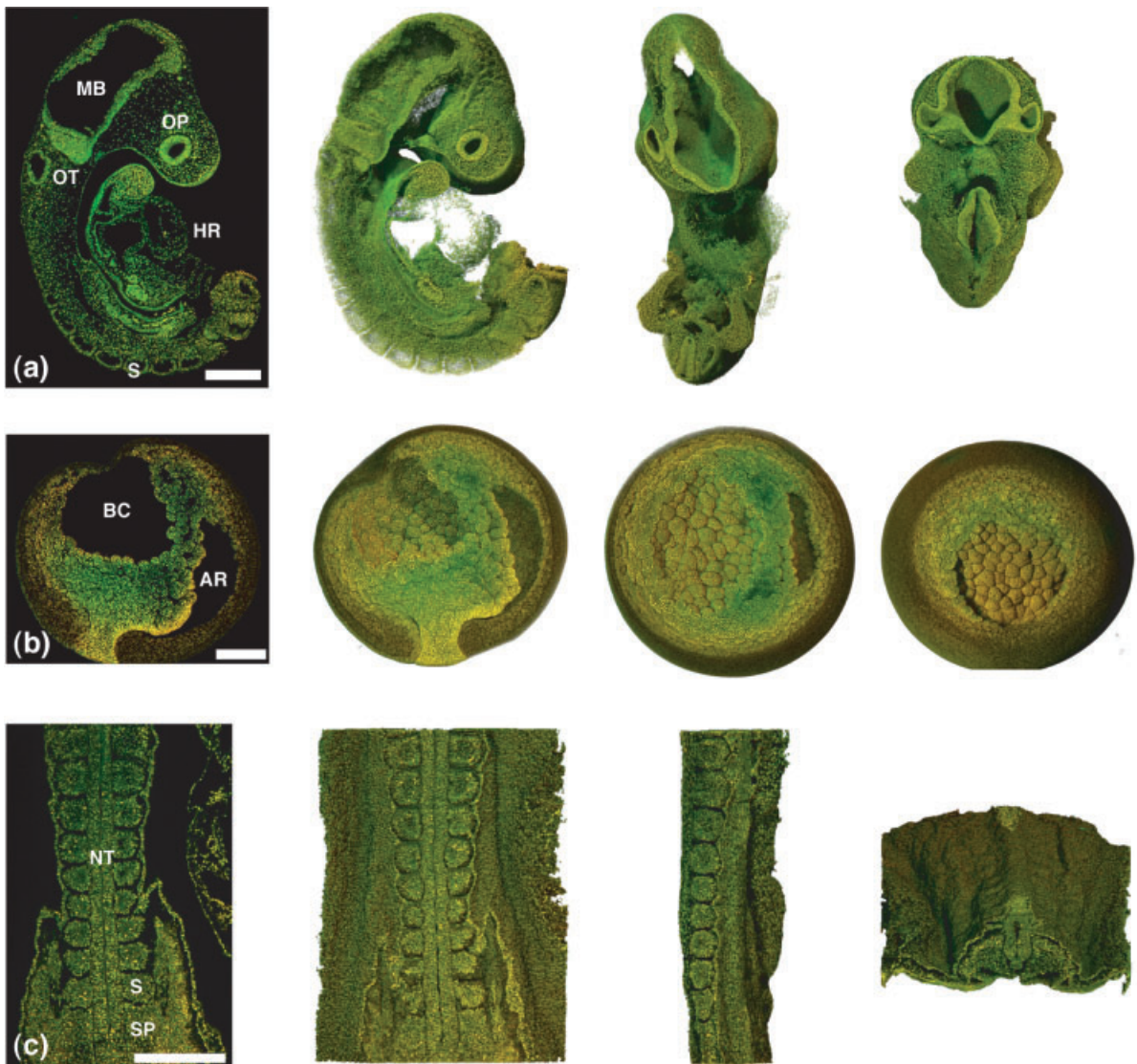


Figure 5.

Several techniques exist that intrinsically collect 3D volumes, rather than 2D sections. Among them are optical coherence tomography (OCT), magnetic resonance imaging (MRI), and optical projection tomography (OPT). OCT images backscattered light coming off a sample, and the technique has the potential to image 3 mm into a living specimen but does so with 12- to 15-micron resolution and few options for specific contrast (Boppart et al., 1996). High-field MRI is excellent for imaging large specimens at 50- to 100-micron resolution. In fixed specimens, 35- to 50-micron resolution is achievable with long scan times and large magnetic fields (Dhenain et al., 2001). OPT is an exciting new technique related to computed tomography that images fixed large samples that have been made optically transparent. OPT is unsuited for embryos that contain very dense tissues such as cartilage or bone, though, and the technique has not been reported at cellular resolution (Sharpe et al., 2002). It is currently a very exciting period in biological imaging, with rapid improvements being made across all imaging modes. SIM aids this progress by filling an unserved niche of cellular resolution on large samples and should prove a highly complementary alternative to existing approaches.

Comparison of SIM With Confocal Laser Scanning Microscopy

To directly compare the performance of confocal laser scanning microscopy (CLSM) (Pawley, 1995) with surface imaging microscopy, we imaged the same propidium iodide-stained chick embryo with both techniques. The in-plane 2D images in Figure 4 (marked x - y) allow assessment of the image quality of the raw data in each imaging mode and show comparable image quality. The most striking differences are the shrinkage of structures in the SIM images, due to dehydration, and the larger overall field of view of the SIM images, which is due to the larger field of view of the surface imaging microscope compared with the Zeiss 410 CLSM. The shrinkage of tissue in alcohol is unavoidable, and the shrinkage we observe is consis-

tent with published norms (Schreibman and Presnell, 1997).

The more informative views of the sample are the orthogonal x - z and y - z views through the resulting 3D volume. The quality of the confocal images clearly falls off very quickly as a function of depth within the sample, even with the use of a water immersion C-Apochromat 10 \times objective lens. Even in regions of the volume where the quality is adequate, the through-plane resolution is worse than the in-plane resolution. SIM, by contrast, has uniform image quality throughout the volume and has indistinguishable resolution and level of detail in the three directions. SIM in-plane image quality is not a function of depth or of the scattering, density, or degree of labeling of the tissue above or below the current plane of optical section. This strategy has a trivial basis, in that there is no overlying tissue, but has profound consequences for image and data set quality.

Practical Resolution of SIM Data Sets

SIM can be performed on a variety of sample sizes and magnifications. These magnifications provide a useful resolution and field-of-view range that brackets whole embryos at tissue resolution through small tissue segments at subcellular resolution. Low (2–4 \times) magnification allows ready identification of tissues and organs within small organisms and enables the study of their morphologic development and relative orientation with respect to each other. Intermediate (10 \times) magnification enables the study of tissues at cellular or subcellular resolution. High (20–40 \times) magnification enables the study of small blocks of tissue at cellular or subcellular resolution.

Range of Systems Tested

Figure 5 depicts 2D raw sections and 3D reconstructions of an intact mouse and frog embryo and a segment of a chick embryo at 10 \times magnification. SIM routinely provides high-resolution, high-contrast images throughout embryos from each of these species at a wide range of stages. The cells of the mouse embryo in Figure 5a are clearly visible, and mesenchymal tissue is quite distinct from epithelial cell layers. This level of resolution provides a clear view of the relationship between developing tissues and organs in the context of an intact embryo. The gastrula stage frog embryo in Figure 5b is composed of relatively large cells, whose shapes and polarities are quite evident in 3D reconstruction, especially those of the cells lining the blastocoel and archenteron. Additionally, the germ layer organization of the frog is quite evident, in the concentric epithelial shells surrounding the vegetal yolk mass. We have imaged chick embryos from Hamburger and Hamilton stage 4–16, frogs from stage 9–22, and mouse embryos from embryonic day 8.5–15.

CONCLUSIONS

We have demonstrated a new imaging technique based on the automated serial collection of thin optical

Fig. 5. Volumetric images of embryos from three model systems. A broad range of sample types are readily imaged using surface imaging microscopy, including chick, mouse, and frog embryos. All three embryos were stained with Resolution Standard stain. **a:** A two-dimensional (2D) raw image collected from a 9.5 days postcoitum (dpc) mouse embryo and three orthogonal three-dimensional (3D) reconstructions of the resulting data set, corresponding to sagittal, transverse, and frontal perspectives. Note the excellent preservation of luminal structures in the midbrain (MB), the somites (S), the heart (HR), the optic vesicle (OP), and the otic vesicle (OT). **b:** A 2D raw image collected from a stage 12 frog embryo and 3D reconstructions of this late gastrula frog embryo, highlighting the blastocoel (BC) and the archenteron (AR). Note the reconstruction of the cell shapes on the floor of the blastocoel and in the lining of the archenteron. **c:** A 2D raw image and three orthogonal 3D reconstructions of a trunk segment from a 16-somite stage chick embryo described in Figure 2. Note the clear developmental progression of somites (S), extending from the segmental plate (SP), adjacent to the neural tube (NT). Scale bars = 250 microns in a–c.

sections from the freshly cut surface of a fluorescently labeled sample embedded in a highly opaque polymer. The realignment accuracy is subresolution, and there is little or no detectable variation in image quality throughout the volume. The voxels of the data set are highly isotropic, allowing digital resampling of the data set from arbitrary virtual planes of section. This technique works across an order of magnitude in sample size and resolution, with improvements on track to significantly extend this range. SIM provides a unique combination of large sample size with high resolution and specific contrast.

We have demonstrated, in three different vertebrate model systems, that the practical resolution of a surface imaging microscope is sufficient to image small blocks of tissue with subcellular detail, large blocks of tissue with cellular resolution, and whole embryos with cellular to tissue resolution. We have also established that SIM produces high-contrast, high-resolution, high signal-to-noise ratio images with five different fluorescent dyes. Finally, direct comparisons, on the same block of tissue, demonstrate the advantages of SIM vs. confocal microscopy, particularly in terms of depth of penetration and maximal sample size.

We expect that the combined ease of review of the primary data and ease of transfer of data should allow SIM to provide novel opportunities for collaborations in which phenotypes can be rapidly evaluated and extensively analyzed by experts at different institutions. The digital 3D models that result from SIM data sets can also be used as a structural scaffold to integrate other categories of information (Streicher and Muller, 2001).

Future technical challenges within the reach of SIM include imaging green fluorescent protein expression in intact embryos, imaging antibody revealed protein expression, and fluorescent in situ hybridization to mRNA probes. We have already achieved some success imaging the clonal distribution of fluorescent dextrans within frog embryos. Improvements in optical sensitivity and whole-mount labeling techniques should enable these advances in the near term. We are also currently working on developing organic dye labeling approaches capable of revealing the plasma membranes of cells throughout the embryo. In combination with the nuclear dyes that have proven successful in this study, these techniques should enable clear visualization of all of the cells in intact vertebrate embryos. Biological problems that we expect SIM to address to in the near future include somitogenesis, gastrulation, and organ morphogenesis. In each case, complex morphogenetic rearrangements are taking place throughout large regions of the embryo, and a cellular level of detail is required to understand the process.

EXPERIMENTAL PROCEDURES

Sample Preparation

White Leghorn chicken eggs were incubated at 37°C for 2 to 3 days until they reached the desired stage of development, typically 16–25 somites. They were then harvested into ice-cold Howard Ringer's solution and

fixed overnight in fresh 4% paraformaldehyde (PFA) at 4°C. After fixation, the embryos were washed three times for 30 min each in phosphate buffered saline (PBS). Embryos of *Xenopus laevis* were obtained, cultured, and dejellied according to standard techniques (Sive et al., 2000). Staging was done according to the Nieuwkoop and Faber normal tables of *Xenopus* development (Nieuwkoop and Faber, 1994). Embryos were cultured to the desired stage, fixed in Bouin fixative (75% picric acid, 25% formaldehyde [37–40%], 5% glacial acetic acid) overnight, and rinsed exhaustively in (50% ethanol, 50% water with 50 mM NH₄OH). The frog embryos were then dehydrated to absolute ethanol, stored overnight in a –20°C freezer, changed to fresh ethanol, and rehydrated to PBS. Embryos from B6D2F1 hybrid mice were obtained from timed matings for which noon of the day when the copulatory plug was found is designated as 0.5 days postcoitus (dpc). Embryos were harvested into ice-cold PBS and transferred into fresh 4% paraformaldehyde for fixation overnight at 4°C. Embryos were rinsed in PBS, dehydrated to 100% ethanol, and rehydrated to PBS.

Sample Labeling

Embryos were fixed in 4% PFA, rinsed in PBS, stained in either propidium iodide (50 µg/ml for 1 hr), DAPI (10 µg/ml for 1 hr), Syto 62 (1:50 dilution for 1 hr), or Topro3 (1:50 dilution for 1 hr) (all from Molecular Probes). Samples labeled with Resolution Standard stain (Resolution Sciences Corporation, Corte Madera, CA) were stained for 6 hr. Dilutions were into PBS. Under all staining conditions, embryos were rinsed in PBS then dehydrated to either methanol or ethanol.

Comparison to Confocal Microscopy

Chick embryos were fixed and stained in propidium iodide (50 µg/ml for 1 hr), then imaged in PBS on a Zeiss 410 confocal microscope, using a C-Apochromat 10× water immersion objective lens. Image acquisition was 512 × 512 pixels, with the pinhole at 1 Airy unit, in-plane resolution at 1.7 microns, and 1.7-micron intervals between optical sections. The embryos were then restained in propidium iodide and imaged by SIM with a 10× Plan Apochromat air objective lens, with 1.77-micron cubic isotropic voxels. Both image stacks were imported into the LSM 510 imaging software, version 3.0 (Carl Zeiss, Inc., Thornwood, NJ), and all comparisons were made therein.

Sectioning and Imaging

To prepare a sample for SIM imaging, it needs to be labeled, fixed, dehydrated, infiltrated, and embedded. We have imaged samples fixed in PFA (4% paraformaldehyde in PBS, pH 7.4), formalin, Carnoy's fixative, and Bouin fixative (Schreibman and Presnell, 1997). Samples have been dehydrated to methanol, ethanol, or isopropanol. This flexibility in sample preparation enables customization to the specific needs of different tissue specimens, allowing for more optimal preserva-

tion of cellular detail and tissue integrity. Additionally, SIM is ideally suited to samples of varying density as it is able to section through dense and loose tissue with minimal chatter or unevenness.

Under all staining conditions, embryos were rinsed in PBS, then dehydrated to either methanol or ethanol. After dehydration, embryonic tissues were equilibrated with a mixture of Resolution Standard embedding polymer and Resolution Standard opacifier (Resolution Sciences Corporation) for 6 hr to allow for cellular infiltration. Opacifier is added to polymer to 82% of saturation to form 100% stock opacified polymer (SOP), which may be stored in aliquots at -4°C for up to 3 months. Before embedding, the SOP is brought to room temperature and then a working polymer is produced by adding to the 100% SOP sufficient additional fresh unopacified polymer to produce the final opacifier concentration appropriate to a given microscope objective. These concentrations have been empirically determined for a set of standard tissues; typical values for different objective lenses are $2\times = 10\%$, $4\times = 20\%$, $10\times = 30\%$, $20\times = 40\%$, $40\times = 50\%$ opacity (Nikon Plan Apochromat series objective lenses). The embedding polymer was cured for 8 hr at 70°C .

The embedded tissue was mounted onto a vertically oriented translation stage assembly, which draws the sample over the edge of a diamond knife, removes the section with vacuum, then repositions the block face in its original location, in the field of view of a Nikon E600 fluorescence microscope with a Plan Apochromat $4\times$, $10\times$, or $20\times$ objective lens. Images were collected to a Kodak Megaplug Model 4.2i charge-coupled device (CCD) camera. Wavelength selection is accomplished with interference filters and dichroic beam splitters (Chroma Corporation, Brattleboro, VT). Individual images were reassembled into a 3D volume that can be visualized and quantified on Resolution ResView 3.1 software. Alternatively, a series of 2D images can be re-exported and computationally reconstructed into a 3D volume that can be manipulated in other image processing programs. Because of the high inherent contrast between the sample and the block face, and the absence of a significant out-of-plane component in the image, there is no need for automated or manual deconvolution techniques to reconstruct accurate 3D renderings from SIM data sets. The entire imaging process, from loading the block to finishing image collection, takes approximately 3 to 6 hr, depending on the number of sections that need to be cut.

ACKNOWLEDGMENTS

We thank Paul Guthrie, Michael Bolles, Michael Haugh, Benn Herrera, and all of Resolution Sciences Corporation, for useful conversations and technical assistance. We also thank David Koos and John Wallingford for useful conversations and David Crotty and Mary Dickinson for providing mouse embryos. A.J.E., H.M., and S.E.F. served as occasional consultants to Resolution Sciences Corporation during the development of this technology. We thank Resolution Sciences Corporation for generously donating instrument time for this project. A.J.E. is a participant in the Initiative in Computational Molecular Biology, which is funded by an award from the Burroughs Wellcome Fund Interfaces Program. H.M. is supported by an NIH NRSA Postdoctoral Fellowship.

REFERENCES

- Boppart SA, Brezinski ME, Bouma BE, Tearney GJ, Fujimoto JG. 1996. Investigation of developing embryonic morphology using optical coherence tomography. *Dev Biol* 177:54–63.
- Brune RM, Bard JBL, Dubreuil C, Guest E, Hill W, Kaufman M, Stark M, Davidson D, Baldock RA. 1999. A Three-dimensional model of the mouse at embryonic day 9. *Dev Biol* 216:457–468.
- Dhenain M, Ruffins SW, Jacobs RE. 2001. Three-dimensional digital mouse atlas using high-resolution MRI. *Dev Biol* 232:458–470.
- Hegre ES, Brashear AD. 1946. Block surface staining. *Stain Technol* 21:161–164.
- Nieuwkoop PD, Faber J, editors. 1994. Normal table of *Xenopus laevis* (Daudin). New York: Garland Publishing, Inc. 252 p.
- Odgaard A, Andersen K, Melsen F, Gundersen HJG. 1990. A direct method for fast three-dimensional serial reconstruction. *J Microsc* 159:335–342.
- Pawley JB, editor. 1995. Handbook of biological confocal microscopy. New York: Plenum Press. 632 p.
- Postlethwait SN. 1962. Cinematography with serial sections. *Turtoc News*. p 98–100.
- Schreibman MP, Presnell JK. 1997. Humason's animal tissue techniques. Baltimore: The Johns Hopkins University Press Ltd. 572 p.
- Sharpe J, Ahlgren U, Perry P, Hill B, Ross A, Hecksher-Sorensen J, Baldock R, Davidson D. 2002. Optical projection tomography as a tool for 3D microscopy and gene expression studies. *Science* 296:541–545.
- Sive HL, Grainger RM, Harland RH. 2000. Early development of *Xenopus laevis*: a laboratory manual. Cold Spring Harbor: Cold Spring Harbor Laboratory Press. 338 p.
- Streicher J, Muller GB. 2001. 3D modelling of gene expression patterns. *Trends Biotechnol* 19:145–148.
- Streicher J, Weninger WJ, Mueller GB. 1997. External marker-based automatic congruencing: a new method of 3D reconstructions from serial sections. *Anat Rec* 248:583–602.
- Toga AW, Ambach KL, Quinn B, Shankar K, Schluender S. 1996. Postmortem anatomy. In: Mazziotto JC, editor. Brain mapping, the methods. San Diego: Academic Press. p 471.
- Weninger WJ, Mohun T. 2002. Phenotyping transgenic embryos: a rapid 3-D screening method based on episcopic fluorescence image capturing. *Nat Genet* 30:59–65.